Mecánica Computacional Volúmen XIII
Compilado por M. Vénere
Bariloche, setiembre de 1992

DENDRITIC SOLIDIFICATION UNDER ELECTROMAGNETIC STIRRING

Sergio D. Felicelli

Centro Atómico Bariloche, 8400 Bariloche, Argentina

ABSTRACT

A mathematical model of dendritic solidification is extended to the magnetohydrodynamic field, by adding Maxwell's equations for the electromagnetic field, coupled with the equations of transport of momentum, energy and solute, through the Lorentz's force term. The evolution of fraction of solid, concentrations in both phases, temperature and velocities during solidification, is calculated using as an example a Pb-Sn system. It is found that if the intensity and frequency of the applied field are chosen appropiately, the macrosegregation can be diminished when compared with an alloy solidified without magnetic stirring.

RESUMEN

Se extiende un modelo matemático numérico de solidificación dendrítica al terreno magnetohidrodinámico mediante el agregado de las ecuaciones de Maxwell para el campo electromagnético, acopladas con las ecuaciones de transporte de momento, energía y soluto a través del término de fuerza de Lorentz. Utilizando como ejemplo un sistema de Pb-Sn, se calcula la evolución de la fracción de sólido, las concentraciones en ambas fases, la temperatura y las velocidades durante la solidificación. Se encuentra que si se elige apropiadamente la intensidad y frecuencia del campo aplicado, puede disminuirse la macrosegregación resultante, comparada con el caso de una aleación que es solidificada sin agitación

1. INTRODUCTION

When a molten alloy is poured into a cooled mold, solidification that grows from the mold walls does not show in general a flat solid/liquid interface. Instead a two-phase region with dendritic or columnar structure is observed, where the primary dendrite arm spacing is very small, of the order of 0.1 mm, depending principally on the solidification velocity[1].

Even if the alloy is initially at uniform composition, the solute will redistribute during solidification leading to a solid with sometimes large inhomogeneities at the macroscopic scale, defect known as macrosegregation.

Many numerical and experimental works[2-5] have consistently shown that macrosegregation is mainly due to thermosolutal convection occurring during solidification. When a liquid alloy is poured into the mold and cooled from the sides, a strong thermal convection is set up almost immediately. As the solidification proceeds, the solid phase generally rejects solute into the interdendritic liquid and solutal convection does also take place. Both of these convective motions contribute to the net solute transport, and therefore to macrosegregation.

If in addition to the thermosolutal effects, convection is also produced by external forces, the macrosegregation pattern can be altered considerably. In the case of electromagnetic stirring (EMS), the external force is the Lorentz's force, originated by the movement of the liquid conductor in a magnetic field. The magnetic field is produced by induction coils placed around the mold. The calculation of macrosegregation during EMS has potential application in many metallurgical processes, such as the continuous casting of steel, where external stirring is applied to induce the growth of an isotropic equiaxial zone instead of the largely directional columnar grains that usually result from solidification without EMS.

Although the physical concept behind EMS is simple, its implementation can present several basic and engineering problems that if not properly resolved can lead to further segregation defects[6,7]. Numerical simulation appears here as a useful tool to analyze the effect of the magnetic field on the convection of the liquid metal and the solute transport. In particular, a careful selection of the intensity, direction and frequency of the applied magnetic field, and of the placement of the inductors, can allow a greater control of the convection occurring during solidification. However, the numerical models currently found in the literature[8,9] only handle the magnetohydrodynamic aspects of the problem coupled with the phase change, and therefore they cannot predict macrosegregation. This task requires a more general model, described in the next section, that also includes the equations of solute and energy transport, in a frame of dendritic solidification.

2 - MATHEMATICAL MODEL

The mathematical model proposed to perform calculations of macrosegregation induced by electromagnetic stirring is an extension of an existing model of dendritic solidification, which was presented in Refs. [5] and [10]. In this model the dendritic or mushy zone is mathematically treated as a porous medium of variable porosity. The porosity is given by the volume fraction of liquid, ϕ, which varies from cero (all-solid region) to one (all-liquid region). A unique set of governing equations is solved in the whole domain with no interface boundary conditions. The equations in the mushy zone automatically reduce to the governing equations for the all-liquid or all-solid regions as the fraction of liquid varies from one to cero, respectively. This type of model, known as continuum model, has also been used by other authors[4]. The unknowns to be calculated are the fraction of liquid, compositions of solute in both phases, temperature, velocities and the magnetic field. Assuming a newtonian and incompressible fluid, laminar flow, and constant and equal physical properties in both phases, the governing equations can be written as follows[10-12]:

1) Conservation of mass:

$$\nabla \cdot \mathbf{u} = 0 \tag{1}$$

where **u** is the superficial velocity, defined as:

$$\mathbf{u} = \phi \mathbf{u}_\ell$$

being $\mathbf{u}_\ell$ the velocity of the interdendritic liquid and ϕ the volume fraction of liquid.

2) Conservation of momentum:

$$\phi \frac{\partial (\mathbf{u}/\phi)}{\partial t} + \mathbf{u} \cdot \nabla(\mathbf{u}/\phi) = -\frac{\phi}{\rho_0}\nabla p + \nu_0 \nabla^2 \mathbf{u} - \nu_0 \phi \mathbf{K}^{-1}\mathbf{u} + \phi \frac{\rho}{\rho_0}\mathbf{g} + \frac{1}{\rho_0}\mathbf{J} \times \mathbf{B} \tag{2}$$

where $$\rho = \rho_0\left[1 - \beta_T(T - T_0) - \beta_C(C - C_0)\right] \tag{2a}$$

In Eqs. (2) and (2a) ρ is the density, ρ_0 is the density in a reference state, β_T is the thermal expansion coefficient, β_C is the solutal expansion coefficient, (T_0, C_0) are the temperature and the concentration in the reference state, p is the pressure, ν_0 is the kinematic viscosity of the liquid, **K** is the permeability tensor of the porous medium (dendritic zone), **g** is the gravity vector, **J** is the electric current density, and **B** is the magnetic field. The last term of Eq. (2) is known as Lorentz's force. The permeability **K** is anisotropic and its components are functions of the fraction of liquid and the dendrite spacing.[10] When $\phi = 1$, the permeability **K** is infinite, the Darcy's term vanishes, and Eq. (2) reduces to the corresponding equation for the all-liquid zone.

3) Equations of the electromagnetic field.

$$\nabla \times \mathbf{E} + \frac{\partial \mathbf{B}}{\partial t} = 0 \qquad \text{Faraday's law} \tag{3a}$$

$$\nabla \times \mathbf{B} = \mu_0 \mathbf{J} \qquad \text{Ampere's law} \tag{3b}$$

$$\mathbf{J} = \sigma(\mathbf{E} + (\mathbf{u}/\phi) \times \mathbf{B}) \qquad \text{Ohm's law} \tag{3c}$$

where **E** is the electric field, σ is the electric conductivity of the liquid, and μ_0 is the magnetic permeability of the vacuum. It is assumed that the alloy is above the Courie's temperature, so that its magnetic permeability μ is equal to μ_0. In Eq. (3b) the term corresponding to displacement currents has been neglected.[13]

From equations (3a-c) we can obtain a unique equation for the magnetic field **B**:

$$\frac{\partial \mathbf{B}}{\partial t} = \nabla \times \left((\mathbf{u}/\phi) \times \mathbf{B} \right) + \frac{1}{\mu_0 \sigma} \nabla^2 \mathbf{B} \tag{3d}$$

Also, using Ampere's law (3b), the Lorentz's force term $\mathbf{J} \times \mathbf{B}$ in the momentum equation can be written as:

$$\mathbf{J} \times \mathbf{B} = -\frac{1}{\mu_0} \mathbf{B} \times (\nabla \times \mathbf{B}) \tag{3e}$$

In this way we have added the magnetohydrodynamic part to the original solidification model through the addition of only one unknown, the magnetic field **B**, whose coupling with the other governing equations is given by equations (3d) and (3e).

4) Conservation of energy:

$$\frac{\partial T}{\partial t} + \mathbf{u} \cdot \nabla T = \alpha \nabla^2 T - \frac{L}{c_s} \frac{\partial \phi}{\partial t} \tag{4}$$

where T is the temperature (taken as equal in both phases), L is the latent heat, c_s is the specific heat and α is the thermal diffusivity.

5) Conservation of solute:

$$\frac{\partial \overline{C}}{\partial t} + \mathbf{u} \cdot \nabla C_\ell = D \nabla \cdot (\phi \nabla C_\ell) \tag{5a}$$

Eq. (5a) is derived stating a solute balance in a volume element that contains solid and liquid. The element is large enough so that its fraction of liquid is equal to the local average, but small enough to be treated as a differential volume. In a similar way, we can obtain the energy equation, Eq. (4).

In Eq. (5a), C_ℓ is the concentration of solute in the liquid phase of the differential volume, while $\overline{C}$ is the total concentration:

$$\overline{C} = \phi C_\ell + (1-\phi)\overline{C}_s \tag{5b}$$

where $\overline{C}_S$ is the average concentration in the solid. An assumption implicit in equation (5a) is that the solute enters and leaves the volume element only by convection in the liquid and by diffusion in the liquid. However there can be diffusion within the local solid. Eqs. (5a-b) must be solved for each one of the alloy components whose macrosegregation is to be calculated. The most simple case is the one of a binary alloy, to be considered in this work.

6) Phase diagram relations

In dendritic solidification of alloys, the local (in a volume element) composition of the interdendritic liquid is essentially uniform, and the solid-liquid interface is very close to equilibrium[14]. It can then be assumed that the composition of the interdendritic liquid is given by the liquidus line of the phase diagram of the alloy, i.e.:

$$C_\ell = \begin{cases} C_L(T) & \text{if } \phi < 1 \\ \overline{C} & \text{if } \phi = 1 \end{cases} \tag{5c}$$

where $C_L(T)$ is the equation of the liquidus. This direct relation between C_ℓ and T is only used in the mushy zone; in the all-liquid region ($\phi = 1$) C_ℓ is calculated from the diffusion-convection balance stated in Eq. (5a).

From the assumption of local equilibrium at the solid-liquid interface:

$$C_S^* = k C_\ell \tag{5d}$$

where C_S^* is the concentration (mass fraction of solute) of the solid at the interface and k partition ratio. Depending on the degree of diffusivity of the solute in the solid, we can make here one of the following approximations: a) Infinite diffusion, where the average concentration of the solid $\overline{C}_S$ is equal to C_S^*; or b) No diffusion, and the resulting microsegregation must be computed as:

$$\overline{C}_S = \frac{1}{g_S}\int_0^{g_S} C_S^*(\eta, t)\,d\eta \tag{5e}$$

where $g_S = 1-\phi$, η is the local fraction of solid coordinate $(0 \le \eta \le g_S)$, and the values of C_S^* are the previous interfacial concentrations in the volume element since it began to solidify $(\eta = 0)$ until the current fraction of solid $(\eta = g_S)$. Assumption b) is suitable for example for a Pb-Sn alloy; while for a Fe-C system, assumption a) should be used. In the more general case of finite diffusion in the solid, we must add a diffusion equation for the solid phase, and the time variation of C_S^* of already solidified elements must be calculated before using Eq. (5e).

The differential equations were discretized using a finite element method based on rectangular bilinear Lagrangian elements. The numerical model uses a Petrov-Galerkin formulation for the convected dominated transport and a penalty function approximation to impose incompressibility.
The algorithm is similar to the one used in the original solidification model[10], plus the addition of the equation for the magnetic field **B** in the iteration loop.

3 - NUMERICAL SIMULATIONS

Results are presented for the directional solidification of a Pb-10wt pct Sn alloy, which shows how the driving force of the electromagnetic stirring can be used to control or diminish the channel segregation commonly observed in vertically solidified castings.

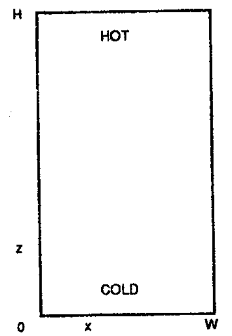

Fig. 1. Domain and coordinate system

A rectangular mold (Fig. 1) is initially filled with a melt of Pb-10 wt pct Sn alloy subjected to a linear temperature distribution, varying from 577 K (just above the melting point) at the bottom to 586 K at the top (the initial thermal gradient is 10 K/cm). The container is 10 mm wide by 20 mm high. The side and top boundaries are insulated and the bottom boundary is cooled at a rate of 1 K/min.

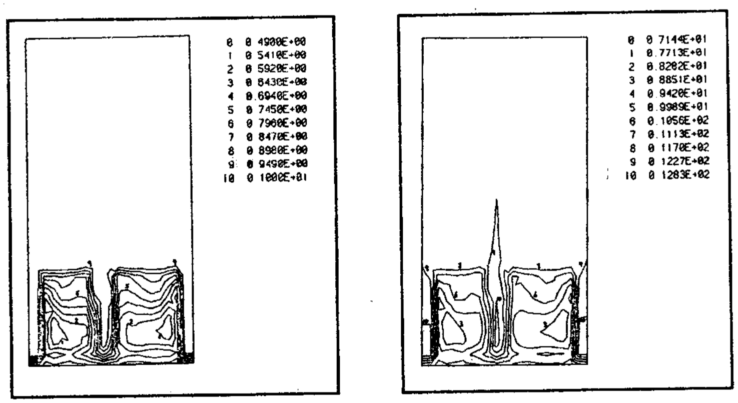

(a) (b)

Fig. 2 - Contour lines of fraction of liquid (a) and total concentration (b) for vertical solidification of a Pb-10wt pct Sn alloy without electromagnetic stirring. Time= 4 min.

After 4 minutes of solidification, the formation of three channels, two at the side walls and one in the interior, is observed (Figs 2a-b). Fig. 2a shows contour lines of fraction of liquid, and a contour diagram of total concentration is shown in Fig. 2b. The liquid in the channels is enriched in solute (Sn) and has therefore a lower freezing point. As explained in Ref. [5], these channels are formed by upward flow of enriched liquid caused by thermosolutal convection.

The same simulation is repeated applying a magnetic field at the side boundaries, of the form

$$\vec{\mathbf{B}}(z,t) = B_0\sqrt{z}\cos\omega t\,\breve{\mathbf{e}}_x \qquad \text{at } x = 0, W$$

In this case the dominant term of the Lorentz's force (Eq. 3e) is proportional to $\left|B\,\partial B/\partial z\right|$ in the $-z$ direction, and is independent of z. The range of penetration of this force decays approximately[15] as $e^{-\frac{x'}{\delta}}$, where $\delta = \sqrt{2/\omega\sigma\mu_0}$, x' is the distance form the boundary, ω is the aular frequency and σ is the electrical conductivity. The idea is to adjust the intensity and frequency of the magnetic field so as to produce a downward force in a region close to the side walls, that opposes the solutal bouyancy force.

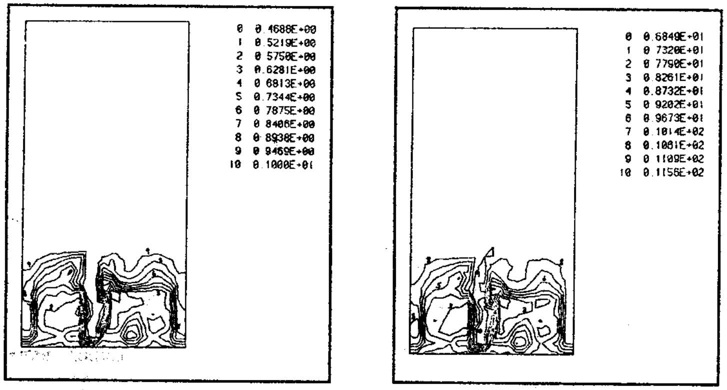

(a) (b)

Fig. 3 - Contour lines of fraction of liquid (a) and total concentration (b) for vertical solidification of a Pb-10wt pct Sn alloy with lateral EMS. Time= 4 min.

Figs. 3a-b show that the action of the magnetic field has reduced the fraction of liquid and the excess of solute concentration in the wall channels. When no EMS is applied, the interdendritic liquid in this region shows concentrations up to 12.8 wt pct, while this value reduces to about 11.5wt pct when the magnetic field is present. This calculation is for only 4 min of solidification, the reduction of segregation can be greater for longer solidification times. Also, no attempt to eliminate the side channels completely has been made. Because the action of the magnetic field is limited to a region close the the side boundaries, the convection in the interior of the mold is not affected considerably and the third channel (in the middle of the container) remains. On the other hand, channel segregation on the outer surface of the casting is usually the most severe. This is so because, during solidification, solute tends to accumulate close to the mold walls, where it is more difficult to be carried away by convection. This originates an upward flow (assuming a solute lighter than the solvent) carrying enriched liquid from the bottom of the mushy zone. The magnetic stirring in the wall region produces a downward driving force that opposes the upward flow and helps to avoid accumulation of solute in this region.

The calculations presented illustrate how the driving force of the electromagnetic stirring can affect the convection occurring during solidification, and the resulting macrosegregation. The model can be used to determine the necessary intensity, frequency and distribution of the magnetic field that produce a more favorable convection pattern, or calculate the macrosegregation for a given location and characteristics of the stirrers. Further calculations of electromagnetic stirring during solidification of other alloy systems in different geometries are in progress.

ACKNOWLEDGEMENTS

This work was partially supported by CONICET under grant PIA 117/90.

REFERENCES

1. KURZ, W. and FISHER, D.J. - "*Fundamentals of Solidification*". Trans Tech Publications LTD, Switzerland, 1986.
2. MEHRABIAN, R., KEANE, M. and FLEMINGS, M.C. - Experiments on Macrosegregation and Freckle Formation, *Metall. Trans.*, **1**, 3238-3241 (1970).
3. SAMPLE, A. and HELLAWELL, A. - The Mechanism of Formation and Prevention of Channel Segregation during Alloy Solidification, *Metall. Trans. A*, **15 A**, 2163-2173 (1984).
4. BENNON, W.D. and INCROPERA, F.P. - A Continuum Model for Momentum, Heat and Species Transport in Binary Solid-Liquid Phase Change Systems - I. Model Formulation, *Int. Journal Heat and Mass Transfer*, **30**, 2161-71 (1987).
5. FELICELLI, S.D., HEINRICH, J.C. and POIRIER, D.R. - Simulation of Freckles during Vertical Solidification of Binary Alloys, *Metall. Trans. B*, **22B**, 847-859 (1991).

6. HURTUK, D.J. and TZAVARAS, A.A. - Some Effects of Electromagnetically Induced Fluid Flow on Macrosegregation in Continuously Cast Steel, *Metall. Trans. B*, **8B**, p. 243 (1977).
7. BRIDGE, M.R. and ROGERS, G.D. - Structural Effects and Band Segregate Formation during the Electromagnetic Stirring of Strand-Cast Steel, *Metall. Trans. B*, **15B**, p. 581 (1984).
8. SPITSEK, K. et al - Rotational Electromagnetic Stirring in Continuous Casting of Round Strands, *Metall. Trans. B*, **17B**, p. 119 (1986).
9. KOSOVIC, B. et al - Freezing under the Influence of a Magnetic Field: Computer Simulation, *Proceedings of the 1991 ICHMT International Symposium on Heat and Mass Transfer in Biomedical Engineering*, Editors: K. Diller, A. Shitzer and S. Siderman, Hemisphere Publishing Corporation, Athens, Greece, September 2-6, 1991.
10. FELICELLI, S.D., HEINRICH, J.C. and POIRIER, D.R. - "Numerical Model for Dendritic Solidification of Binary Alloys", *Num. Heat Transfer*, accepted.
11. FELICELLI, S.D. - "*Simulation of Freckles during Vertical Solidification of Binary Alloys*", Ph.D. Dissertation, The University of Arizona, Tucson, Arizona, 1991.
12. FELICELLI, S.D. - Cálculo de Macrosegregación durante Agitación Electromagnética en Colada Continua", Internal Report, Centro Atómico Bariloche, Bariloche, 1992.
13. JACKSON, J.D. - "*Classical Electrodynamics*", 2nd. edition, John Wiley & Sons, 1975, Ch. 10.
14. FLEMINGS, M.C. - "*Solidification Processing*", McGraw-Hill Book Co, New York, NY, 1974, pp. 141-146.
15. HAMMOND, P. - "*Applied Electromagnetism*", Pergamon Press, Oxford, UK, 1978.